



Multi-View Extraction of Dynamic Pedestrian Density Fields

MATTHIAS PLAUE, MINJIE CHEN, GÜNTER BÄRWOLFF & HARTMUT SCHWANDT, Berlin

Keywords: density estimation, human crowd analysis, pedestrian flows, velocimetry, video analysis

Summary: In the framework of macroscopic models of human crowds, pedestrian dynamics are described via local density and flow fields. In this paper, we expand our previous work on the extraction of pedestrian trajectories and density fields from video recordings of crowd experiments in two ways. Firstly, we include data from different video cameras in order to cover a larger observation area. Secondly, we improve our previous density estimation method by introducing a new kernel function which (a) yields density fields that are also differentiable functions in time and (b) models the influence of multiple neighbouring pedestrians on the personal space of an individual.

We apply this density computation method to pedestrian trajectories extracted from video data of a crowd experiment conducted by us, and compare the results with other common methods for density computation in this context: a technique based on Voronoi diagrams, and a fixed-bandwidth estimator. We come to the conclusion that the technique proposed by us combines advantages from both alternative methods, yielding spatio-temporally smooth density fields close to the standard definition of density at all scales.

Zusammenfassung: *Multiperspektivische Erfassung dynamischer Dichtefelder von Fußgängern.* Makroskopische Modelle zur Beschreibung von Personenbewegungen greifen auf Konzepte wie lokale Dichte- oder Flussfelder zurück. In einer früheren Arbeit haben wir ein Verfahren beschrieben, durch das individuelle Trajektorien sowie Dichtefelder mithilfe von Videoaufnahmen von Experimenten mit Personenströmen erfasst werden können. Dieses Verfahren wurde in zweierlei Hinsicht erweitert bzw. verbessert: Zum einen können Videodaten aus mehreren Kameras dazu verwendet werden, einen größeren Beobachtungsbereich abzudecken. Zum anderen kann unsere Methode der Dichteschätzung durch Verwendung einer anderen Kernfunktion verbessert werden. Der so erhaltene Schätzer liefert Dichtefelder welche (a) bzgl. des Zeitparameters differenzierbare Funktionen darstellen und (b) den Einfluss mehrerer benachbarter Personen auf den von einem Individuum eingenommenen Raum modellieren.

Mithilfe dieser Methode berechnen wir Dichtefelder auf Grundlage von Trajektorien, welche aus Videoaufnahmen eines von uns durchgeführten Fußgängerexperiments gewonnen wurden. Das Resultat vergleichen wir mit zwei in diesem Kontext gebräuchlichen Methoden zur Dichteberechnung: einem auf Voronoi-Diagrammen basierenden Verfahren sowie einem Kerndichteschätzer mit konstanter Bandbreite. Wir kommen zu dem Schluss, dass mit unserem Ansatz Vorteile der beiden alternativen Methoden vereint werden, indem die Berechnung raumzeitlich glatter Dichtefelder ermöglicht wird, welche auf allen Skalen standardmäßig berechnete Dichtewerte approximieren.

1 Introduction

The study of pedestrian dynamics has important applications in crowd management such as devising strategies for the evacuation of

buildings or public places. In order to evaluate the predictive power of mathematical models designed to emulate human crowd behaviour, it is a common procedure to compare numerical simulations based on these models with empirical data.

Furthermore, different modelling approaches demand the extraction of different types of data: For example, the social force model (HELBING & MOLNÁR 1995) and cellular automaton model (BURSTEDDE et al. 2001) aim at predicting pedestrian trajectories, whereas continuum methods adopted from fluid mechanics (HUGHES 2002) describe the dynamics via the density and flow of the crowd. In our work, we develop models based on these three approaches in order to simulate intersecting pedestrian flows and compare these simulations with the real world. Here, we describe one important part of this work: the extraction of the trajectories and a dynamic, continuous density field from video recordings of human crowd experiments. The work presented here is an extension of PLAUE et al. (2011).

1.1 Challenges and Contribution

In section 2, we describe an experiment that was conducted with the purpose of demonstrating the dynamic behaviour of intersect-

ing pedestrian flows (Fig. 1). To this end, we set up an experiment where two unconfined, perpendicularly intersecting pedestrian flows have been recorded by multiple cameras with overlapping fields of view. To the best of our knowledge, no such experiment has previously been conducted.

In that section, we also describe a semi-automated technique to extract the spatio-temporal positions of pedestrians in a crowd of low density at close range from an arbitrary observation angle. Due to constructional limitations, it was not possible to install the cameras to provide a bird's eye view. This situation is very different from most experimental setups found in the common literature, where a bird's eye view installation of the camera(s) in sufficient height provides an advantageous perspective. In some studies, the heights of the pedestrians are also indicated by visual markers, which also greatly facilitate automated pedestrian tracking (BOLTES et al. 2010). Having neither bird's eye views nor markers, we devised a method to extract the floor positions of the pedestrians without knowing their re-

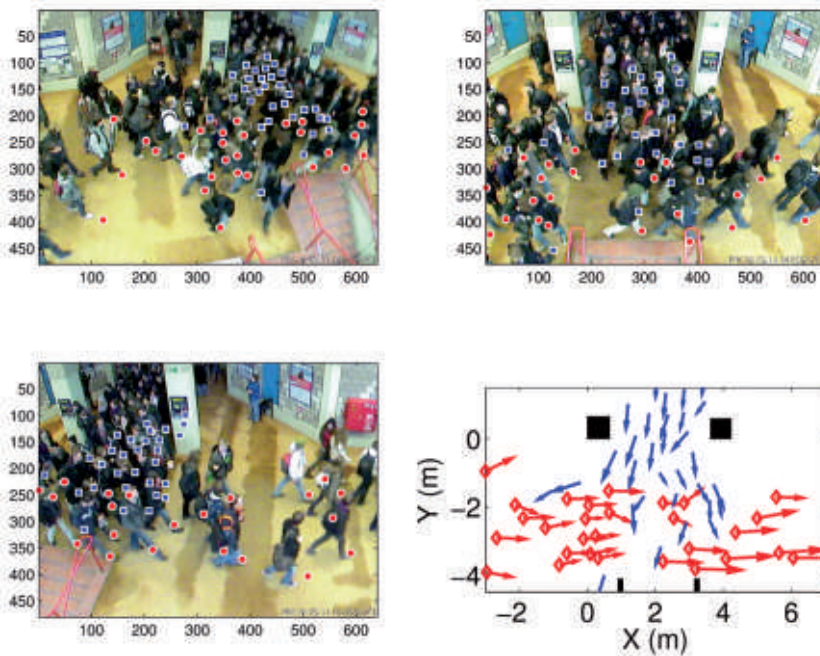


Fig. 1: Human crowd experiment from three different observation points. Bottom right: extracted pedestrian positions at time step $t = 68.2$ s of group A (red diamonds) and group B (blue). Arrows indicate current velocity; the maximal length corresponds to 1.4 m/s.

spective body heights beforehand. Furthermore, we perform a fusion of data from multiple video cameras.

The estimation of the density field of a sparse crowd is a challenging task because of the low number of samples. In section 3, we propose a novel method to compute a high-resolution smooth density field from the spatio-temporal positions of the pedestrians based on a kernel density estimator with variable bandwidth. In that section, we also give a comparison of our results with other density estimators. Finally, an overview of future work will be given in section 4.

1.2 Related Work

Human crowd experiments

Empirical data for the evaluation of human crowd models are usually extracted from video recordings of either naturally occurring crowds (HELBING et al. 2007) or pedestrian flows that have been produced under controlled conditions (DAAMEN & HOOGENDOORN 2003, GALEA et al. 2011, ZHANG et al. 2011). In general, the latter are devised to demonstrate crowd behaviour in special situations such as evacuation or passage through a bottleneck. In our work, we wish to analyze the dynamics of intersecting pedestrian flows. A very similar experiment with this purpose has been conducted by GUO et al. (2010); however, data from only one camera was processed in that case. Also, in our experiment, the pedestrians did not move along specified, confined corridors.

(Semi-) automatic pedestrian tracking

There exists a large body of literature on methods for the detection and automatic tracking of humans. The range of application of such algorithms varies greatly. For example, SCHMIDT & HINZ (2011) address the problem of tracking the positions of pedestrians from aerial images which provide very low resolution, and CREMERS (2006) proposes a method to track the contour of an individual through noise and occlusion. For an overview on different methodologies, we refer to HU et al. (2004).

In this work, we follow the suggestion of BOLTES et al. (2010), who process video data similar to ours, and use the Lucas-Kanade algorithm (SHI & TOMASI 1994) to facilitate the extraction of the spatio-temporal positions of the pedestrians. Additionally, we employ an algorithm to merge the trajectories from different overlapping camera views via the Hungarian method (KUHN 1955, MUNKRES 1957). Note that we merge the trajectories *after* processing the video data, in contrast to the detection of objects from multiple views during tracking (see for example KAHN et al. 2001).

Pedestrian density estimation

Probably the most basic way to compute a density would be to divide the number of pedestrians in a given region by the area of that region, at a given point in time. However, this “standard” density estimator is not a smooth point-wise density function and yields data with large scatter.

At least two approaches for measuring the (local) density of human crowds have been suggested in the literature as alternatives:

- In HELBING et al. (2007), a local density field is computed via the sum of Gaussians with fixed standard deviation (typically 0.7 m) centred at each pedestrian. Formally, this approach is identical to kernel density estimation with fixed bandwidth, which is a basic tool in statistical data analysis (see SILVERMAN 1986, for example). This method yields a smooth density field defined at every point.
- In STEFFEN & SEYFRIED (2010), estimators are proposed based on the Voronoi diagram defined by the position of each pedestrian as a Voronoi site. The main idea in this approach is to account for the personal space occupied by each pedestrian, and this personal space is represented by the area of the corresponding Voronoi cell. The values for the Voronoi density are very close to standard densities, but with a significantly smaller scatter. However, the Voronoi estimator does not yield a smooth local density defined at every point.

The algorithm that we propose here is conceptually a combination of the Voronoi esti-

mator (accounting for personal space) and the fixed-bandwidth kernel estimator (yielding smooth density fields).

2 Experiments and Trajectory Extraction

In the following, we describe human crowd experiments that we conducted in the lobby of the Department of Mathematics building of Technische Universität Berlin in December 2010, and the extraction of the trajectories of the participants from video streams captured by several cameras.

2.1 Experimental Setup

In the experiment which we use to illustrate our method, two pedestrian flows (group *A*, 142 subjects, and group *B*, 83 subjects) intersected at an angle of 90 degrees for one minute in a region of about 25 m², reaching a peak density of about five pedestrians per m². The scene was recorded from a gallery at a height of about 6 m with five networked and temporally synchronized JVC VN-V25U surveillance video cameras. Here, we will analyze the data provided by the three central cameras which covered the area where the actual intersecting of the pedestrian flows took place (Fig. 1).

2.2 Extraction of Spatio-Temporal Positions

For camera calibration, we assumed a pinhole model and estimated the model parameters by measurement of the world and image coordinates of about 30 fixed reference points in the scene. For each camera, this procedure resulted in a camera matrix, and thus enabled us to deduce the parameters of a homography between the camera's image plane and the floor. The video data have been analyzed in a semi-automatic manner for each camera as described in the following (see also PLAUE et al. 2011). Our main goal is the supervised extraction of reliable data.

1. The video is played back frame by frame. Image segments corresponding to the heads of pedestrians that newly enter the scene are marked manually. These templates are used to determine the head positions in the next frame via the Lucas-Kanade tracking method (SHI & TOMASI 1994). Based on the difference of spatial positions in consecutive frames as well as the residual i.e., difference between the detected texture and the template, an error score is computed for each person. If this score is too high or the user spots a possible tracking error regardless of the score, the head position/template can be corrected manually.
2. Once the image coordinates of the heads of the pedestrians have been determined, the video is played again from the beginning. For each pedestrian in the frame, the head position is shown together with the corresponding floor position, initially under the assumption that every pedestrian has a standard height of $h = 1.70$ m. In each frame the user may correct the floor position of a pedestrian by simply clicking into the frame, and the current height and floor position coordinates are updated via the homography determined in camera calibration.
3. Each pedestrian is assigned a final height value equal to either the arithmetic mean of the height values from the corrections in step 2, or equal to the standard height $h = 1.70$ m if no user instruction for this pedestrian is available during this step. Based on this final height value and the image coordinates of the head, in each frame we compute the world coordinates $(X, Y, 0)$ of each pedestrian's position on the floor.

Remarks

- In our scenario, the floor position of most of the pedestrians is visible at some point in time, for example before entering or exiting the crowded intersection area. Therefore, manual correction of the floor position is feasible.
- In order to improve the user's corrections of the floor positions it might be reasonable to provide a view of all cameras and the respective positions during step 2.
- One might introduce/implement a pattern recognition module to carry out the func-

tion of an automatic marker. However, even if the whole algorithm provided a fully automatic analysis, manual verification would nevertheless be good experimental practice in order to obtain reliable data.

2.3 Merging Trajectories from different Camera Views and Smoothing

The above procedure yields the positions of the pedestrians on the floor covered by each camera. Originally the cameras were positioned so that these floor areas overlapped. However, it was not immediately possible to merge the trajectories since they are not labelled as individual pedestrians. To solve this problem, we implemented the following algorithm:

1. For each pair of pedestrians captured by different cameras, compute their distance in each frame. Compute the mean value across the frames. Due to measurement errors, this value does not vanish even if it is computed for the same pedestrian captured by two different cameras. However, we expect the mean distance to be minimal if the same pedestrian is captured by two different cameras. If two pedestrians do not appear together in at least one frame, a very large distance value is assigned to this pair of pedestrians. If one camera captures fewer pedestrians than the other, pedestrians very far away will be added to this data set to yield a square distance matrix.
2. The problem to find the permutation of labels that yields the minimal distance for each pair of pedestrians is a combinatorial optimization problem that we solve with the Kuhn-Munkres algorithm, also known as the Hungarian method (KUHN 1955, MUNKRES 1957). Data that cannot be assigned automatically can be assigned manually, or be discarded. In our case, data from about 15 pedestrians had to be managed in this way.
3. Due to systematic errors such as lens distortion and due to errors in the measurement process, the positions of the pedestrians from the cameras on the side show a displacement with respect to those obtained from the central view. We use the central view as a reference and shift the positions

from the cameras on the side towards the corresponding positions from the central camera for the differences between the locations in different videos to be minimized after merging the data. Finally, for each pedestrian, all available data points are approximated by cubic B-splines to yield smooth trajectories ($t, X(t), Y(t)$). By differentiating these trajectories with respect to the time parameter t , the velocities of the pedestrians can be easily computed (Fig. 1).

A frame of the analyzed video sequence can be seen in Fig. 1. Since we use the central camera as the reference view in step 3 above, measurement errors are particularly visible in the camera views from the side. One can see that in this particular scene, the positions of some pedestrians located near the intersection area are not marked. This is due to the fact that these pedestrians could not be reliably assigned a trajectory over a sufficiently extended time period, and therefore were discarded. Note that with the currently available image size of 640×480 pixels, it proves difficult to trace individual pedestrians in a very crowded scene, even for an attentive human observer. In our earlier experiments, we bypassed this problem by equipping the subjects with coloured clothing hoping to establish a better visual contrast.

3 Variable-Bandwidth Kernel Density Estimation

In the following, we describe and investigate a novel method for kernel density estimation. We apply this technique to compute a density field from the trajectories of the pedestrians.

3.1 Definition

Consider a Gaussian kernel density estimator with variable bandwidth to compute the density at time t and position \mathbf{x} :

$$\rho(t, \mathbf{x}) = \frac{1}{2\pi} \sum_{i \in \mathcal{J}} \frac{1}{(\lambda d_i(t))^2} \exp\left(-\frac{\|\mathbf{x}_i(t) - \mathbf{x}\|^2}{2(\lambda d_i(t))^2}\right). \quad (1)$$

Here, J denotes an index set labelling the pedestrians, and λ is an additional dimensionless smoothing parameter. The bandwidth $\lambda d_i(t)$ is estimated from the trajectories $\mathbf{x}_i(t)$ of the pedestrians – the formal analogy in statistical data analysis is also known as a sample smoothing estimator (TERRELL & SCOTT 1992). For example, assuming $\lambda = 1$, for the nearest-neighbour kernel estimator (PLAUE et al. 2011),

$$d_i(t) = \min_{j \in J, j \neq i} \|\mathbf{x}_i(t) - \mathbf{x}_j(t)\|. \quad (2)$$

However, this kernel and therefore the total density are not differentiable with respect to time. Furthermore, it does not account for the fact that the personal space of a pedestrian is affected not only by the nearest pedestrian but also by other pedestrians in the immediate vicinity. Therefore, we propose the following alternative:

$$d_i^{(p)}(t) = \left(\sum_{j \in J, j \neq i} \|\mathbf{x}_i(t) - \mathbf{x}_j(t)\|^{-p} \right)^{-1/p}. \quad (3)$$

This is a smooth function and at the same time generalizes the nearest-neighbour kernel as its limiting case of $p \rightarrow \infty$.

3.2 General Properties and Parameters

In Fig. 2, a toy-model calculation for a single pedestrian is shown in order to demonstrate how the bandwidth is determined by multiple neighbouring pedestrians for reasonable val-

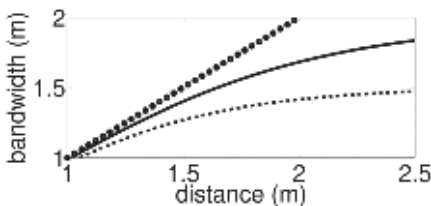


Fig. 2: The bandwidth, defined by (3) with $p = 4$, assigned to a particular pedestrian A as a function of the distance to another individual pedestrian B . Dotted line: with no other pedestrian present. Solid line (dashed line): with one other pedestrian C (three other pedestrians C , D and E) located at a constant distance of two metres to A .

ues of the parameters p and λ . For large values of the parameter p , the bandwidth only depends on the nearest neighbour. For small values of p , the bandwidth is a function of all nearby pedestrians, and it decreases with the number of nearby pedestrians. Therefore, this parameter defines the degree to which other nearby pedestrians influence personal space.

Fig. 3 shows the density field computed with this kernel at a particular point in time. By comparison with the fixed-bandwidth estimator, this figure also illustrates how the variable-bandwidth estimator distributes “pedestrian mass” to favour densely crowded regions. We would like to note that this feature is consistent with a model assumption that is frequently found in the description of pedestrian dynamics (“chemotaxis”): interactions between pedestrians are repulsive for short distances and attractive for longer distances (see for example SCHADSCHNEIDER et al. 2002). Also, we expect the proposed density estimator is useful for the visualization of other types of data, in particular if one is interested in highlighting clusters. For large values of the parameter λ , the density field becomes more spatially smoothed and less “fine-grained”, distributing pedestrian mass more broadly.

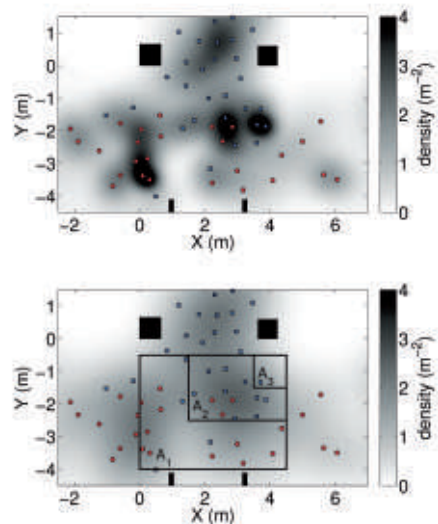


Fig. 3: Top: pedestrian density field, computed with the kernel defined by (3) with $\lambda = 1$, $p = 4$; bottom: computed with a fixed bandwidth of $d = 1$ m. Black indicates a density > 4 m^{-2} .

3.3 Comparison with other Density Estimators

In Fig. 4, a plot of the density versus time is shown, averaged over the regions marked in Fig. 3, and computed by four methods: the standard method of counting people in the region, a fixed-bandwidth kernel estimator, our variable-bandwidth estimator, and finally the density estimator based on Voronoi diagrams denoted in STEFFEN & SEYFRIED (2010) as “ D_V ”. The regions have the respective areas $A_1 = 15.8 \text{ m}^2$, $A_2 = 6 \text{ m}^2$, and $A_3 = 1 \text{ m}^2$.

Remark

The Voronoi method in its original form is not designed for unconfined crowds; we work around this fact by assuming that the pedestrians stop and cease to move once they exit the area covered by the cameras, thereby limiting the size of the boundary Voronoi cells. More recently, LIDDLE et al. (2011) propose to simply cut off the Voronoi cells beyond a disk

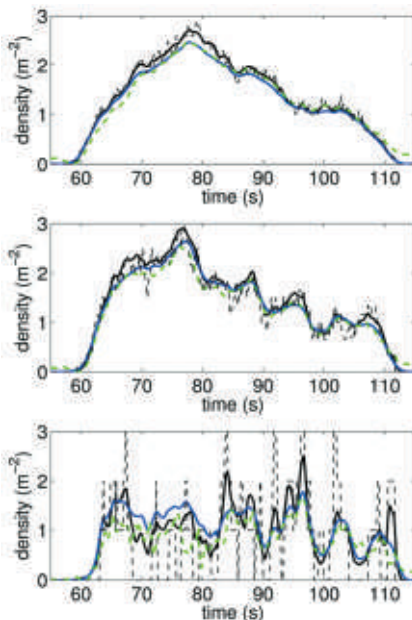


Fig. 4: From top to bottom: pedestrian density, spatially averaged across the areas marked A_1 , A_2 and A_3 in Fig. 3. Kernel density with fixed bandwidth $d = 0.7 \text{ m}$ (blue line), with variable bandwidth (black line), Voronoi density (dashed green line), standard density (thin black dashed line).

of certain radius centred at the respective pedestrian.

All methods yield results very similar to the standard density when computed for very large regions, with the possible exception of the Voronoi estimator (without cut-off) because of boundary cells of infinite size. However, for smaller regions, the fixed-bandwidth estimator typically yields values that are significantly lower than the standard density since a large portion of the pedestrian mass is located outside the respective region. For very small “microscopic” regions, such as A_3 , the densities computed with the fixed-bandwidth estimator can be larger than the standard density since pedestrian mass from outside the region cumulates inside the region regardless of the number of pedestrians already occupying that location. In contrast to this, Fig. 4 demonstrates that the estimator proposed by us yields values that are close to the standard density at all scales. As a result, small temporal variations in density are also described more faithfully by this estimator. Therefore, we may compute pedestrian density data with high spatio-temporal resolution and high precision. We expect that this feature is particularly useful to analyze the fine structure of fundamental diagrams (ZHANG et al. 2011).

4 Conclusion and Future Work

In this work, we present a framework for measuring local density fields from video recordings of human crowds captured by multiple cameras. By utilizing methods from photogrammetric image analysis, we first extract the trajectories of the pedestrians from each camera, and merge these data by matching locations with minimum spatio-temporal distance.

From these trajectories, we compute the pedestrian density field via a modified version of a nearest-neighbour kernel estimator recently proposed by us, with an additional parameter p that serves as a temporal smoothing parameter for the bandwidth. The density obtained in this way is a smooth function of the object coordinates and time, and faithfully represents the standard density when averaged over regions of arbitrary sizes.

In addition, the reader may be aware that the density field is applicable in the estimation of a flow field by requiring that the continuity equation holds. This approach is the subject of present work, the results of which will be reported in PLAUE et al. (2012), where we will also describe how obstacles and boundaries can be taken into account.

Note that the automatic, data-driven estimation of values for p and λ is still an open problem in our context. Methods from statistical data analysis for automatic bandwidth selection might prove to be appropriate tools to attack this problem (COMANICIU 2003, WU 2007).

Acknowledgements

We would like to thank all university staff and students who helped with conducting the experiments, and we especially thank C. NEUMANN for carrying out the data analysis and implementing the density estimation method based on Voronoi diagrams. Furthermore, we thank the reviewers for their helpful comments and suggestions.

The authors gratefully acknowledge the support of Deutsche Forschungsgemeinschaft (German Research Foundation) for the project SCHW548/5-1 + BA1189/4-1.

The numerical calculations were made with the computing software MATLAB by MathWorks.

Finally, we would like to thank the organizers of the conference Photogrammetric Image Analysis 2011, Technical University of Munich, Germany.

References

- BOLTES, M., SEYFRIED, A., STEFFEN, B. & SCHADSCHNEIDER, A., 2010: Automatic Extraction of Pedestrian Trajectories from Video Recordings. – *Pedestrian and Evacuation Dynamics*, PED **2008**: 43–54.
- BURSTEDDE, C., KLAUCK, K., SCHADSCHNEIDER, A. & ZITTARTZ, J., 2001: Simulation of Pedestrian Dynamics Using a Two-Dimensional Cellular Automaton. – *Physica A* **295**: 507–525.
- COMANICIU, D., 2003: An Algorithm for Data-Driven Bandwidth Selection. – *IEEE Transactions on Pattern Analysis and Machine Intelligence* **25** (2): 281–288.
- CREMERS, D., 2006: Dynamical Statistical Shape Priors for Level Set-Based Tracking. – *IEEE Transactions on Pattern Analysis and Machine Intelligence* **28** (8): 1262–1273.
- DAAMEN, W. & HOOGENDOORN, S.P., 2003: Experimental Research on Pedestrian Walking Behavior. – *Transportation Research Board annual meeting*: 1–16.
- GALEA, E.R., FILIPPIDIS, L., WANG, Z., LAWRENCE, P.J. & EWER, J., 2011: Evacuation Analysis of 1000+ Seat Blended Wing Body Aircraft Configurations: Computer Simulations and Full-Scale Evacuation Experiment. – *Pedestrian and Evacuation Dynamics*, PED **2010**: 149–151.
- GUO, R.-Y., WONG, S.C., HUANG, H.-J., ZHANG, P. & LAM, W.H.K., 2010: A Microscopic Pedestrian-Simulation Model and Its Application to Intersecting Flows. – *Physica A* **389**: 515–526.
- HELBING, D. & MOLNÁR, P., 1995: Social Force Model for Pedestrian Dynamics. – *Physical Review E* **51** (5): 4282–4286.
- HELBING, D., JOHANSSON, A. & AL-ABIDEEN, H.Z., 2007: Dynamics of Crowd Disasters: An Empirical Study. – *Physical Review E* **75** (4): 046109.
- HU, W., TAN, T., WANG, L. & MAYBANK, S., 2004: A Survey on Visual Surveillance of Object Motion and Behaviors. – *IEEE Trans. On Systems, Man, and Cybernetics* **34** (C3): 334–352.
- HUGHES, R.L., 2002: A Continuum Theory for the Flow of Pedestrians. – *Transportation Research Part B* **36**: 507–535.
- KHAN, S., JAVED, O. & SHAH, M., 2001: Tracking in Uncalibrated Cameras with Overlapping Field of View. – *Performance Evaluation of Tracking and Surveillance (PETS 2001)*.
- KUHN, H.W., 1955: The Hungarian Method for the Assignment Problem. – *Naval Research Logistic Quarterly* **2**: 83–97.
- LIDDLE, J., SEYFRIED, A., STEFFEN, B., KLINGSCH, W., RUPPRECHT, T., WINKENS, A. & BOLTES, M., 2011: Microscopic Insights Into Pedestrian Motion Through a Bottleneck, Resolving Spatial and Temporal Variations. – [arXiv:1105.1532v1](https://arxiv.org/abs/1105.1532v1) [physics.soc-ph].
- MUNKRES, J., 1957: Algorithms for the Assignment and Transportation Problems. – *Journal of the Society for Industrial and Applied Mathematics* **5** (1): 32–38.
- PLAUE, M., CHEN, M., BÄRWOLFF, G. & SCHWANDT, H., 2011: Trajectory Extraction and Density Analysis of Intersecting Pedestrian Flows from Video Recordings. – *ISPRS Conference on Photogrammetric Image Analysis (PIA 2011)*, LNCS **6952**: 285–296.

- PLAUE, M., BÄRWOLFF, G. & SCHWANDT, H., 2012: On Measuring Pedestrian Density and Flow Fields in Dense as well as Sparse Crowds. – to appear in Proceedings Pedestrian and Evacuation Dynamics (PED 2012).
- SCHADSCHNEIDER, A., KIRCHNER, A. & NISHINARI, K., 2002: Cellular Automaton Approach to Collective Phenomena in Pedestrian Dynamics. – 5th International Conference on Cellular Automata for Research and Industry (ACRI 2002), LNCS **2493**: 239–248.
- SCHMIDT, F. & HINZ, S., 2011: A Scheme for the Detection and Tracking of People Tuned for Aerial Image Sequences. – ISPRS Conference on Photogrammetric Image Analysis (PIA 2011), LNCS **6952**: 257–270.
- SHI, J. & TOMASI, C., 1994: Good Features to Track. – IEEE Conference on Computer Vision and Pattern Recognition: 593–600.
- SILVERMAN, B.W., 1986: Density Estimation for Statistics and Data Analysis. – Chapman and Hall, London, UK.
- STEFFEN, B. & SEYFRIED, A., 2010: Methods for Measuring Pedestrian Density, Flow, Speed and Direction with Minimal Scatter. – Physica A **389** (9): 1902–1910.
- TERRELL, G.R. & SCOTT, D.W., 1992: Variable Kernel Density Estimation. – Annals of Statistics **20** (3): 1236–1265.
- WU, T.-J., CHEN, C.-F. & CHEN, H.-Y., 2007: A Variable Bandwidth Selector in Multivariate Kernel Density Estimation. – Statistics & Probability Letters **77** (4): 462–467.
- ZHANG, J., KLINGSCH, W., SCHADSCHNEIDER, A. & SEYFRIED, A., 2011: Transitions in Pedestrian Fundamental Diagrams of Straight Corridors and T-Junctions. – Journal of Statistical Mechanics **2011** (6): P06004.

Address of the Authors:

MATTHIAS PLAUE, MINJIE CHEN, GÜNTER BÄRWOLFF & HARTMUT SCHWANDT, Technische Universität Berlin, Institut für Mathematik, D-10623 Berlin, Tel.: +49-30-314-25651, Fax: +49-30-314-21110, web page: <http://www.math.tu-berlin.de/projekte/smdpc/>, e-mail: {plaue}{minjie.chen}{baerwolf}{schwandt}@math.tu-berlin.de

Manuskript eingereicht: Februar 2012

Angenommen: Juni 2012